ORGANOMETALLICS
Article
pubs.acs.org/Organometallics

Tracking Intramolecular Interactions in Flexibly Linked Binuclear Platinum(II) Complexes

Ilona Stengel,[†,‡] Cristian A. Strassert,[‡,§] Luisa De Cola,*[,‡,§,∥] and Peter Bäuerle*[,†,‡]

[†]Institute of Organic Chemistry II and Advanced Materials, University of Ulm, Albert-Einstein-Allee 11, 89081 Ulm, Germany
[‡]Dutch Polymer Institute (DPI), P.O. Box 902, 5600 AX Eindhoven, The Netherlands
[§]Center for Nanotechnology and Physikalisches Institut, Westfälische Wilhelms-Universität Münster, Heisenbergstrasse 11, 48149 Münster, Germany

S Supporting Information

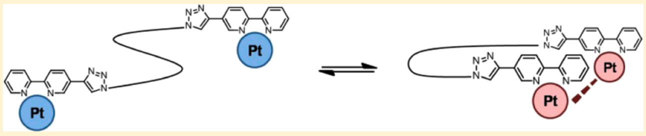

ABSTRACT: In this work we describe the synthesis and the photophysical and electrochemical characterization of binuclear Pt^{II} complexes. Using a modular click chemistry approach, we decorated different flexible bridging units with (bpy)Pt^{II} bisacetylides (bpy = 2,2′-bipyridine). Intramolecular excimer formation originating from Pt^{II}−Pt^{II} and π−π interactions was investigated by steady-state and time-resolved emission spectroscopy in dilute solution. We observed that linkers bringing the metallic centers in close proximity favor both ground-state coupling and excimer formation. These interactions lead to changes in the photophysical and electrochemical properties, which can be tuned by the choice of solvent.

INTRODUCTION

Mononuclear Pt^{II} complexes bearing aromatic ligands show bright luminescence due to emissive intraligand (IL) and metal-to-ligand charge transfer (MLCT) excited states.[1−4] Over the past 20 years, a variety of derivatives has been synthesized and some candidates have been successfully applied in organic light-emitting diodes (OLED) as phosphorescent dopants.[5] In contrast to other luminescent materials such as octahedral Ir^{III} complexes, Pt^{II} compounds display special features due to their square-planar geometry. Stacking interactions in the z direction promoted by close Pt^{II}−Pt^{II} (d_{z^2}−d_{z^2}) and π−π contacts result in significant changes on absorption and emission properties.[6−9]

Such properties were investigated in the solid state for mononuclear Pt^{II} complexes at first.[6] If two Pt^{II} centers are aligned face to face at a distance shorter than 3.5 Å, their d_{z^2} orbitals interact with each other to give one bonding σ and one antibonding σ^* molecular orbital (MO).[6e] Shorter Pt^{II}−Pt^{II} distances give rise to stronger interactions and larger MO splitting, resulting in red-shifted absorption bands due to $d\sigma^*(Pt_2) \rightarrow \pi^*$ transitions defined as metal−metal to ligand charge transfer (MMLCT).[7]

Dilute solutions of mononuclear Pt^{II} complexes usually display ^{1}MLCT and ^{1}IL absorption bands without any additional features, as ground-state Pt^{II}−Pt^{II} interactions are generally too weak to overcome the effect of dilution. However, even if they are monomeric in nature in the ground state, the interactions are much stronger in the excited state and excimer formation is often observed.[7−9] Thus, the intensity of the excimer emission, which increases with the concentration,[8a] is enhanced at the expense of the monomer emission.

Series of binuclear Pt^{II} complexes bearing aromatic ligands and defined close intramolecular Pt^{II}−Pt^{II} distances have been reported to further investigate the effects of metal−metal interaction on the photophysical properties.[10] The correlation between crystal structures and absorption and emission spectra has shown that the lowest energy excited state is shifted to lower energies upon decreasing the intramolecular Pt^{II}−Pt^{II} distance, when different bridging moieties are used. MMLCT absorption bands inbetween 430 and 490 nm with molar extinction coefficients ranging between 2000 and 4000 M^{-1} cm^{-1} have been observed for binuclear Pt^{II} complexes with intramolecular Pt^{II}−Pt^{II} distances of 2.998−3.432 Å.[10b] Some related derivatives appeared to be highly luminescent, with quantum yields of 44% in solution,[11] and some have successfully been used as phosphors in OLEDs.[12]

There are also reports about binuclear Pt^{II} complexes with rigid bridging units providing face to face arrangements at larger Pt^{II}−Pt^{II} distances and preventing metal−metal interaction.[13] Thus, no MMLCT absorption could be monitored; however, broad, intense, and concentration-independent excimeric emission around 700 nm was observed appearing clearly red-shifted, in comparison to signals for analogous mononuclear compounds.[13b] Intramolecular π−π interactions were found to be responsible for this kind of excimer emission, causing similar effects on the profiles of the emission spectra analogously to Pt^{II}−Pt^{II} interactions. Furthermore, it has been suggested that solvent molecules being able to competitively interact with π systems disturb the intramolecular interactions and diminish the excimer emission.[13c]

In the case of flexibly linked binuclear species, an equilibrium of different conformations with and without Pt^{II}−Pt^{II} and π−π interactions is reached in solution.[14−18] It has been revealed

Received: May 14, 2013
Published: March 5, 2014

dx.doi.org/10.1021/om4004237 | *Organometallics* 2014, 33, 1345−1355

Scheme 1. Synthesis of Flexibly Linked Binuclear Pt^{II} Complexes Using Click Chemistry[a]

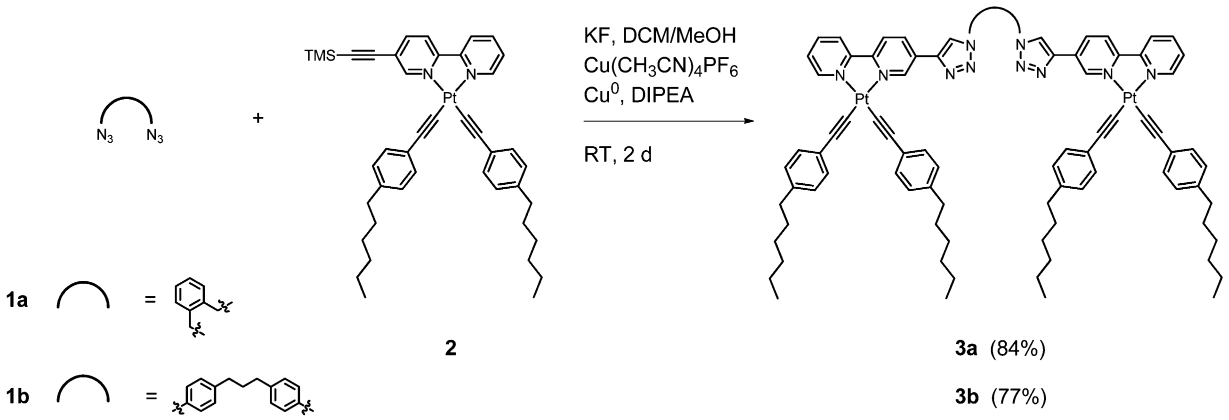

[a]Abbreviations: DCM, dichloromethane; DIPEA, diisopropylethylamine.

Scheme 2. Synthesis of Flexible Linker 1b[a]

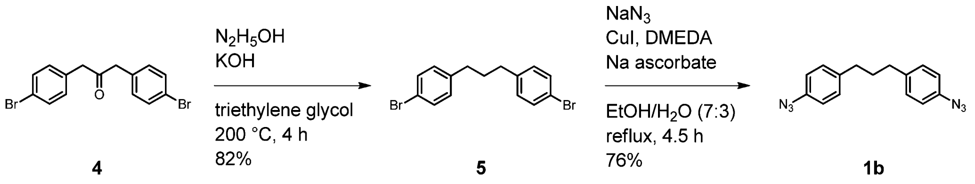

[a]Abbreviation: DMEDA, *N,N′*-dimethylethylenediamine.

Scheme 3. Synthesis of Flexible, Polyethylene Glycol (PEG) Linked Binuclear Pt^{II} Complexes with and without *n*-Hexyl Chains at the Phenylacetylide Ligands

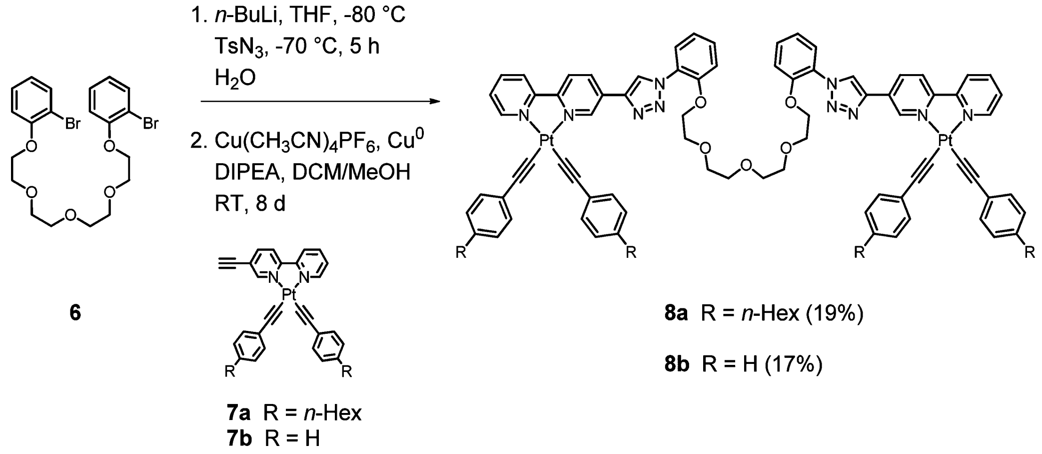

that the length and the steric demand of the linker affect the extent of intramolecular interactions in bisphosphinoalkyl binuclear Pt^{II} complexes.[15] For such compounds, it is hard to distinguish between Pt^{II}−Pt^{II} and $\pi-\pi$ interactions in solution; however, differences have been studied in the solid state.[16] Flexibly linked binuclear (tpy)Pt^{II} complexes (tpy = terpyridine) have been reported to show increasing intramolecular interactions in dilute solution when the temperature is lowered.[17] In this respect, Pt^{II}−Pt^{II} and $\pi-\pi$ interactions resulted in self-assembling properties, which have been studied for a variety of different mono- and binuclear Pt^{II} compounds.[19] Recent examples demonstrated flexible binuclear Pt^{II} complexes, in which the emission could be switched from ^{3}MLCT to ^{3}MMLCT upon changing the pH[20] and the solvent,[21] respectively.

Herein we describe the synthesis of four flexibly linked binuclear Pt^{II} complexes employing click chemistry.[22] Such architectures could show tunable emission properties, provided that the distance between the emitting centers can be controlled. We recently presented the Cu(I)-catalyzed [3 + 2] azide−alkyne cycloaddition (CuAAC) reaction as a versatile method to functionalize luminescent mononuclear Pt^{II} derivatives[23] and now extend the strategy to binuclear Pt^{II} complexes. In order to understand the respective intramolecular interactions, we focused on the photophysical and electrochemical investigation of the obtained compounds.

■ RESULTS AND DISCUSSION

Synthesis. 1,2-Bis(azidomethyl)benzene (**1a**) and 1,3-bis(4-azidophenyl)propane (**1b**) were chosen as linkers for binuclear Pt^{II} complexes (Scheme 1). Diazides **1a**,**b** were each

Chart 1. Structures of Herein Described Binuclear Pt^{II} Complexes 3a,b and 8a,b and Their Corresponding Mononuclear Counterparts M3a, M-3b/8a, and M-8b[23]

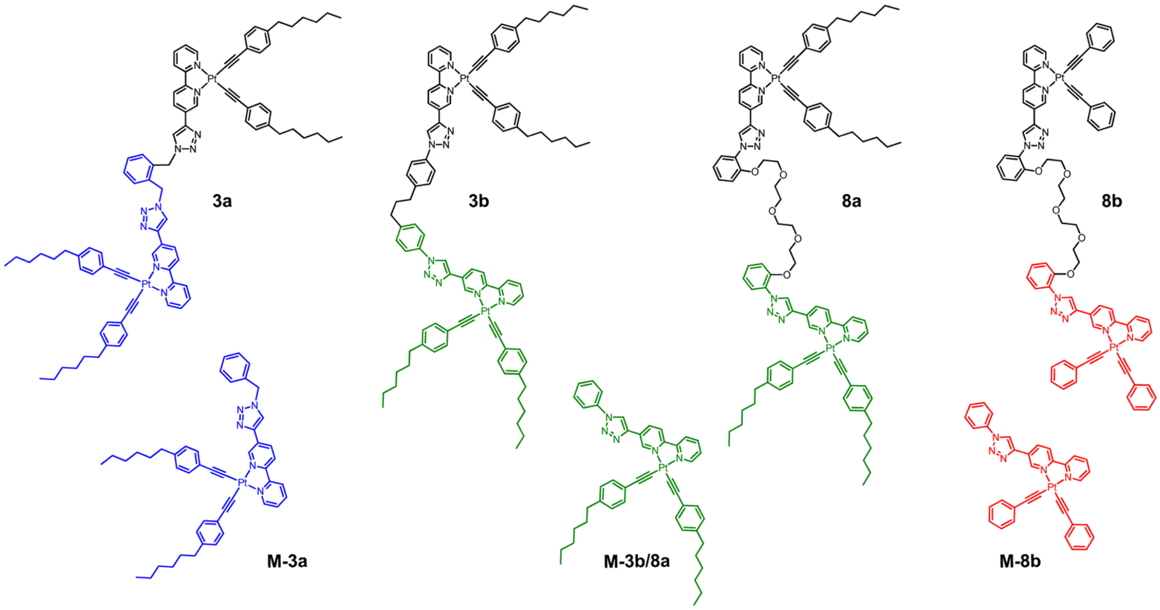

reacted with (5-(TMS-ethynyl)-bpy)Pt^{II} complex **2**,[23] potassium fluoride for in situ deprotection, and Cu(CH_3CN)$_4$$PF_6$ as click catalyst in a dichloromethane−methanol mixture at room temperature. Small amounts of elemental copper were added to rereduce possibly oxidized Cu^{II} species. The synthetic protocol was adopted from our formerly published series of click-functionalized luminescent mononuclear Pt^{II} analogues.[23] Thin-layer chromatography (TLC) showed complete consumption of the starting materials after a reaction time of 2 days. Subsequent aqueous workup, silica column chromatography, and additional size exclusion chromatography (SEC) provided binuclear Pt^{II} complexes **3a,b** in 84% and 77% yields, respectively.

Linker **1a** was synthesized from 1,2-bis(bromomethyl)-benzene and sodium azide in dimethyl sulfoxide (DMSO) at room temperature in a nucleophilic substitution reaction.[24] The synthesis of linker **1b** is depicted in Scheme 2. 1,3-Bis(4-bromophenyl)propan-2-one (**4**) was synthesized according to a protocol known from the literature.[25] The carbonyl group in **4** was reduced in a Wolff−Kishner reaction to the corresponding methylene, giving compound **5** in 82% yield. The bromo substituents in **5** were substituted by azido groups in a Cu(I)-catalyzed aromatic substitution reaction,[26] providing 1,3-bis(4-azidophenyl)propane (**1b**) in 76% yield.

A more flexible bridge, 1,13-bis(2-azidophenyl)-1,4,7,10,13-pentaoxatridecane, between the same Pt^{II} moieties was introduced as the third linker in complex **8a** and was synthesized from its corresponding dibromide **6** (Scheme 3).[27] In this case, Cu(I)-catalyzed aromatic substitution to the corresponding diazide with the method described above did not work in satisfactory yield. Alternatively, lithiation with *n*-butyllithium in THF at −80 °C and subsequent quenching with tosyl azide provided a mixture of the bisazido intermediate and hydrogenated byproducts in a 6:1 ratio.[28] We used this mixture in the subsequent CuAAC reaction with deprotected (5-ethynyl-bpy)Pt^{II} complex **7a**.[23] After aqueous workup and purification using silica and size-exclusion chromatography, binuclear Pt^{II} complex **8a** was obtained in 19% yield (with respect to dibromide **6**). In comparison to the other binuclear complexes **3a,b**, compound **8a** showed better solubility in organic solvents due to the PEG linker.

The corresponding derivative **8b** without hexyl chains at the phenylacetylide ligands was synthesized as well, yielding similar results after the CuAAC reaction. The solubility of complex **8b** in organic solvent was still sufficient. In contrast, attempts to attach (5-ethynyl-bpy)Pt^{II} complex **7b** without solubilizing alkyl chains at the acetylides to diazide linker **1a** only gave an insoluble product. Hence, the CuAAC reaction is a modular synthetic approach to link monometallic Pt^{II} complexes to various functionalized backbones, if adequate solubility of the product is provided by the bridging or ancillary ligands.

The structures of all four bimetallic Pt^{II} complexes **3a,b** and **8a,b** were analyzed by proton NMR, MALDI-TOF mass spectrometry, FT-IR spectroscopy, and elemental analysis or high-resolution MALDI-TOF mass spectrometry. For all compounds, only one set of sharp signals was obtained in the ^{1}H NMR spectrum for each Pt^{II} moiety, confirming the symmetry of the complexes. Most of the chemical shifts are comparable to those of the related mononuclear Pt^{II} analogues **M3a**, **M-3b/8a**, and **M-8b** (Chart 1), respectively, which have been synthesized and characterized previously.[23] However, the triazolyl proton (H-5‴) in **3a** is shifted distinctly upfield to δ 7.00 ppm in comparison to parent mononuclear complex **M-3a** (7.89 ppm). The signals of the benzylic protons are similar in both compounds, whereas the two protons of the bpy ligand adjacent to the triazolyl residue (H-6, H-4) are shifted slightly upfield, indicative of an increased electron density in this part of the molecule. In case of binuclear complex **3b**, the signal of the triazolyl proton is shifted upfield to δ 7.95 ppm in comparison to the parent mononuclear compound **M-3b/8a** (8.39 ppm). However, the shift is not as pronounced as in the case of **3a**/**M-3a**. The bridging unit in **3b** certainly provides a higher degree of flexibility than the bridge in complex **3a**, as indicated in the proton NMR spectrum by a less pronounced upfield shift in comparison to the related mononuclear compound. The ^{1}H NMR spectra of **8a,b** displayed sharp and well-resolved signals

Table 1. Photophysical Data of the Mono- and Binuclear Complexes[a]

complex	λ_{abs} (nm) (ε (M^{-1} cm^{-1}))	λ_{em}[b] (nm)	λ_{em}(DMF)[b] (nm)	λ_{em}(77 K)[b] (nm)	Φ[d]
M-3a	418 (6400)	610	607	544	0.08
M-3b/8a	416 (5900)	618	608	540	0.05
M-8b	413 (6000)	600	595	532	0.19
3a	422 (11500)	605, 755	608, 745	546 (700)[c]	<0.01
3b	413 (11200)	615, 750	610	542	0.02
8a	421 (12900)	601, 750	609	535	<0.01
8b	414 (12400)	595, 750	593	529	<0.01

[a] All measurements were carried out at c[Pt] ≈ 10^{-5} mol L^{-1} in DCM solution at 298 K unless noted otherwise. [b] λ_{ex} 430 nm. [c] Shoulder to the main emission band given in parentheses. Φ denotes the photoluminescence quantum yield. [d] Measured with an integrating sphere; experimental uncertainty ±0.01.

for all moieties in $CDCl_3$ at room temperature, indicating negligible aggregation in solution.

Absorption and Steady-State Emission. The absorption and emission properties of binuclear Pt^{II} complexes **3a**,**b** and **8a**,**b** were investigated in comparison to those of their corresponding mononuclear analogues **M3a**, **M-3b/8a**, and **M-8b**, respectively, at similar Pt^{II} concentrations ($[Pt_2]$ = 2[Pt]) in dichloromethane (DCM) solutions. The photophysical data are summarized in Table 1. All complexes displayed intense absorption bands in the region between 250 and 350 nm with maximum molar extinction coefficients (ε) of up to 99 × 10^3 M^{-1} cm^{-1}, which can be assigned to intraligand $\pi-\pi^*$ transitions centered at the bipyridine and the phenylacetylide units, according to Eisenberg and Che.[3e,g] Additionally, the low-energy bands between 350 and 550 nm show molar extinction coefficients from 11.2 to 12.9 × 10^3 M^{-1} cm^{-1} for the binuclear complexes and half the ε values for the parental mononuclear species (between 5.9 and 6.4 × 10^3 M^{-1} cm^{-1}; see Figures S1−S5 in the Supporting Information). For all compounds the lowest energy absorptions can be attributed to mixed ^{1}MLCT and ^{1}LLCT transitions (metal and phenylacetylide to diimine), according to Castellano et al.[3i,j] Figure 1 shows the normalized absorption spectra of all compounds.

For all the binuclear Pt^{II} complexes comparison with the corresponding mononuclear species, e.g. **3a** and **M-3a** (Figure 1a), shows identical absorption profiles in the lower energy part of the spectrum. Additional red-shifted absorption bands, shoulders, or a broadening of MLCT bands could not be observed for the binuclear compounds. Thus, no hints for intramolecular interactions of the two Pt^{II} units in the ground state can be traced in the absorption spectra of solutions at room temperature. However, we should note that the absorption of the intense ^{1}MLCT bands could hide the presence of weaker aggregate bands.

Complexes **8b** and **M-8b** displayed blue-shifted absorption in comparison to compounds **8a** and **M-3b/8a**, as they lack the electron-donating hexyl chains at the phenylacetylide ancillary ligands.

Absorption measurements in different solvents further support the MLCT assignments of the low-energy bands. Representatively, the absorption spectra of binuclear complexes **3a**,**b** measured in different solvents are depicted in Figure 2a,c, respectively. The lowest energy absorption band of both compounds showed negative solvatochromism, indicating that the polar ground state is increasingly stabilized along with the polarity of the solvent. Consequently, the MLCT band is shifted to higher energies with increasing polarity of the solvent. This effect is well-known for mononuclear (bpy)Pt^{II} bisacetylides.[3i,j]

Interestingly, the emission spectra show strong solvatochromism that does not correlate with solvent polarity. The emission spectra of binuclear complex **3a** in different solvents are depicted in Figure 2b together with the emission spectrum of mononuclear complex **M-3a** in DCM at a comparable concentration of Pt^{II} centers. The mononuclear complex displayed a single, unstructured emission band between 550 and 750 nm with negligible solvatochromism, whereas the binuclear compound **3a** displayed a new emission band at 755 nm in DCM with a shoulder at 605 nm. In DMF and THF, the red-shifted emission of binuclear complex **3a** has a lower intensity.

The emission behavior of the more flexible binuclear complex **3b** is similar. If the emission spectrum of **3b** in DCM is compared to the emission spectrum of the mononuclear counterpart **M-3b/8a** in DCM, an additional shoulder at 750 nm can be monitored (Figure 2d). The red shift is even more intense in a 3/1 DCM/*n*-hexane mixture, whereas no red shift was observed in DMF solution, in which the emission of binuclear complex **3b** appears identical with the emission of the related mononuclear complex **M-3b/8a**.

It is clear that the luminescence of the binuclear species is significantly different from that of the corresponding mononuclear species at the same Pt^{II} concentration, as is shown in Figure 2b,d. In addition, the emission spectra of the binuclear species are not concentration dependent (see Figures S6−S9 in the Supporting Information). The emission bands around 600 nm of both the mono- and binuclear complexes are assigned to a ^{3}MLCT state, in accordance with previously reported data.[3e,g,23] On the other hand, the red-shifted bands with maxima around 750 nm are attributed to excimer emission originating from intramolecular interactions.

The behavior of binuclear complexes **8a**,**b** is comparable to that of derivative **3b**. The corresponding emission spectra are given in the Supporting Information (Figures S10 and S11). Notably, complex **8b**, lacking the hexyl chains at the phenylacetylide ligands, showed a stronger tendency to form excimers in comparison to complex **8a** by displaying more intense red-shifted bands around 750 nm.

These results suggest that intramolecular $Pt^{II}-Pt^{II}$ and $\pi-\pi$ interactions are suppressed by those solvents that are able to competitively interact with the (bpy)Pt^{II} moieties.[13c] Furthermore, these interactions are diminished by sterically demanding substituents at the (bpy)Pt^{II} moieties and longer bridging units.

Moreover, excitation spectra of the mono- and binuclear Pt^{II} complexes, monitored at 600 and 750 nm, showed identical profiles irrespective of the solvent (Figures S14−S19, Supporting Information). This further supports the absence

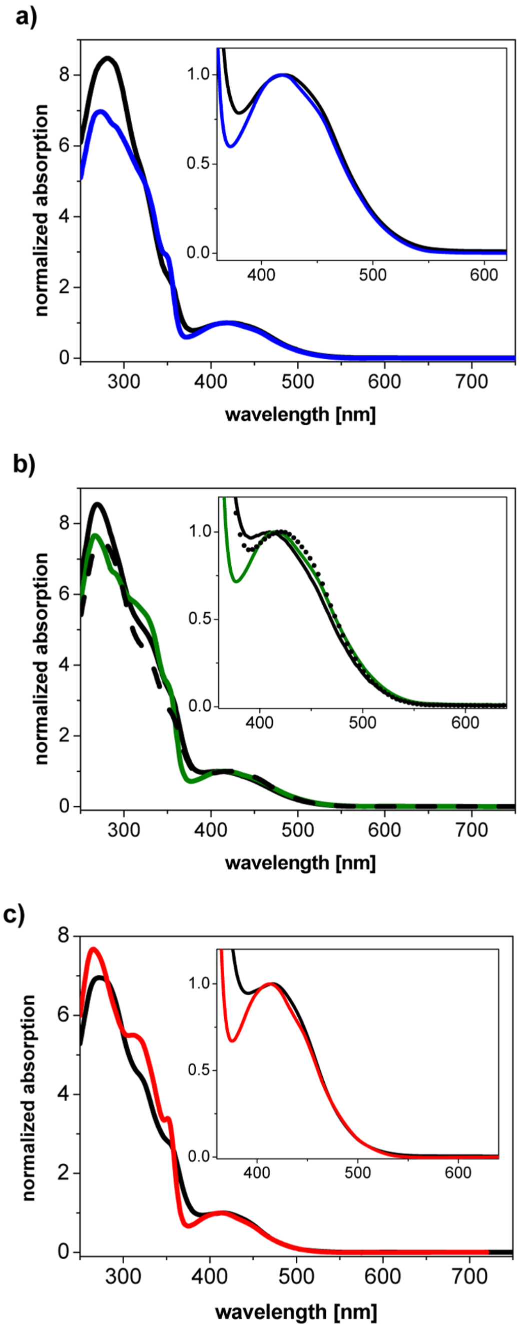

Figure 1. Normalized absorption spectra in DCM solutions at room temperature of binuclear ($c \approx 5 \times 10^{-6}$ M) and their corresponding mononuclear complexes ($c \approx 10^{-5}$ M): (a) binuclear complex **3a** (black, solid line) and mononuclear compound **M-3a** (blue, solid line); (b) binuclear complexes **3b** (black, solid line) and **8a** (black, dashed line) and mononuclear compounds **M-3b**/**8a** (green, solid line); (c) binuclear complex **8b** (black, solid line) and mononuclear compound **M-8b** (red, solid line). Insets: enlargement of the MLCT bands.

of distinct intramolecular ground-state interactions in the binuclear (bpy)Pt^{II} complexes.

In general, the binuclear complexes were not as luminescent as their related mononuclear species. The photoluminescence quantum yields (PLQY) of all binuclear complexes were determined and range from 1 to 2%, whereas comparable mononuclear complexes showed PLQYs spanning from 8 to 19%. Triplet−triplet annihilation as well as the presence of low-lying excited states, rising from intramolecular interactions, are responsible for this behavior.

If the emission of binuclear Pt^{II} complex **3a** is measured in dilute glassy DCM at 77 K, the spectrum appears very similar to that of its mononuclear relative **M-3a** (Figure 3a). In both cases, the slightly structured emission between 525 and 700 nm can be assigned to mixed ^{3}MLCT and ^{3}IL transitions.[23] Additionally, a weak and broad shoulder can be monitored between 650 and 850 nm for binuclear compound **3a**. The excimeric nature of the low-energy emission of **3a** was confirmed by the absence of distinctive excitation maxima at 77 K when monitoring the luminescence at 550 and 675 nm (see Figure S20, Supporting Information). This excimer emission is not apparent for binuclear complex **3b** (Figure 3b) and the even more flexible derivatives **8a**,**b** (Figures S12 and S13, Supporting Information). The fact that the red-shifted emission maximum is diminished at 77 K as in comparison to that at room temperature further points to its excimeric nature.

Time-Resolved Emission. In order to understand the dynamics of excimer formation and its correlation with the nature of the bridging units, we performed wavelength-dependent, time-resolved luminescence decay studies in dilute DCM solution (Table 2). Generally, multiexponential decays were obtained due to the manifold of conformations adopted by the binuclear complexes. As expected, the emissions at shorter wavelengths are mainly related to the relaxation of the mononuclear excited states, whereas the excimer emission is predominant at lower energies. In complex **3a**, the Pt^{II} centers are brought in close proximity by the rather rigid linker, thus facilitating excimer formation. Consequently, only a minor fraction of the Pt^{II} centers decay with a characteristic lifetime corresponding to unperturbed mononuclear Pt^{II} complexes (222 ns),[23] as observed by monitoring the decay at 600 nm. Indeed, most of the Pt^{II} complexes decay with a shortened lifetime of 3 ns, due to the formation of excimeric species. In addition, a minor component corresponding to the onset of the excimer emission (29 ns) is observed. At 770 nm, the most significant component results from the excimer emission (29 ns), showing a rise time of 3 ns that correlates well with the fast decay of the excited Pt^{II} units. An almost negligible emission tail of unperturbed Pt^{II} centers can be traced at 770 nm (222 ns). On the other hand, the more flexible linker employed in complex **3b** provides further degrees of conformational freedom, leading to an additional component (104 ns) due to weakly interacting Pt^{II} moieties (self-quenching). At 770 nm, the characteristic decay of the excimer is again observed (27 ns) with a rise time of 3 ns, along with a significant fraction of only partially quenched Pt^{II} centers (104 ns). These observations indicate that increasing the flexibility and length of the bridging unit results in an enhanced mononuclear-like emission, which was confirmed by the decays of compounds **8a**,**b** clearly showing rise times (7 and 5 ns, respectively) longer than that of **3a**,**b** (3 ns). Steric hindrance of peripheral substituents also plays a role in keeping the Pt^{II} moieties apart, as evidenced by the removal of hexyl chains in complex **8b**.

Electrochemistry. The redox properties of binuclear Pt^{II} complexes **3a**,**b** and **8a**,**b** have been investigated in comparison to their mononuclear analogues. All relevant data are summarized in Table 3. If the cyclic voltammogram (CV) of complex **3a** in DMF is compared to the corresponding CV of mononuclear compound **M-3a** at the same platinum concentration (Figure 4a), it is observed that the reduction potentials are identical for both compounds. The same is true for the

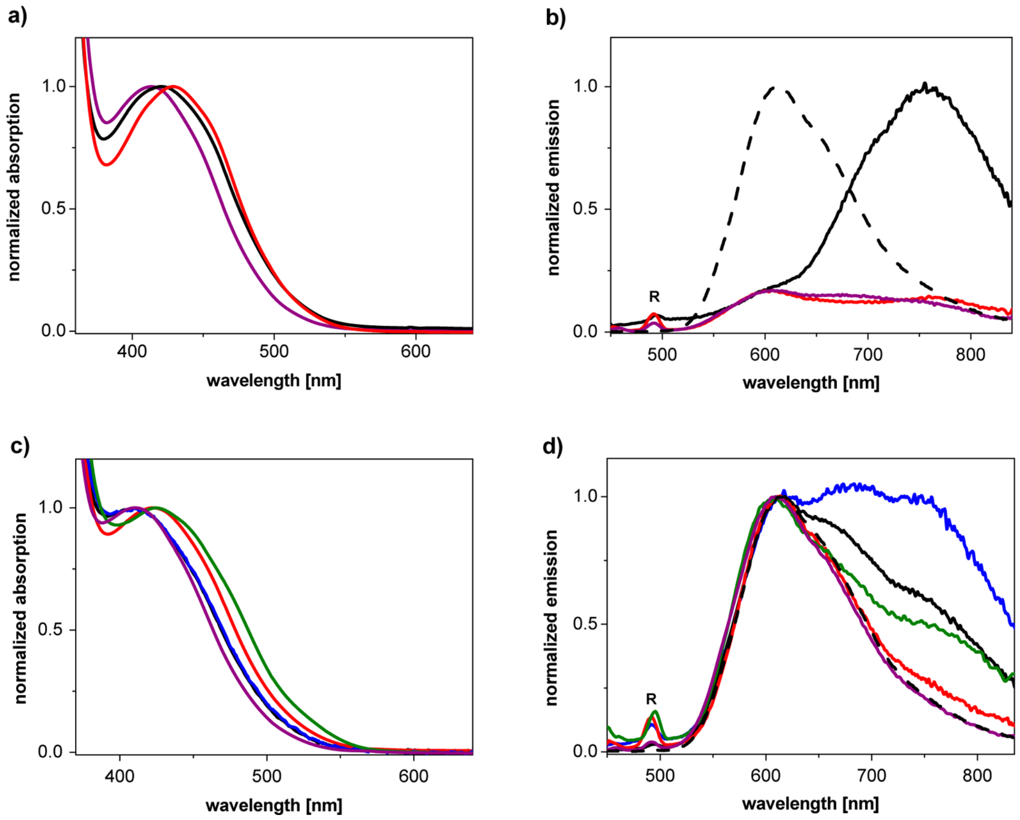

Figure 2. Normalized absorption and emission spectra of binuclear compounds **3a**,**b** ($c \approx 5 \times 10^{-6}$ M) in various aerated solvents, DCM (black), THF (red), DMF (purple), benzene (green), DCM/hexane 3:1 (blue): (a) normalized absorption spectra of **3a** at room temperature; (b) normalized emission spectra of **3a** and of the corresponding mononuclear complex **M-3a** (DCM, dashed line, $c \approx 10^{-5}$ M); (c) normalized absorption spectra of **3b** at room temperature; (d) normalized emission spectra of **3b** and of the corresponding mononuclear compound **M-3b**/**8a** (DCM, dashed line, $c \approx 10^{-5}$ M). The excitation λ_{ex} is at 430 nm; R denotes Raman scattering.

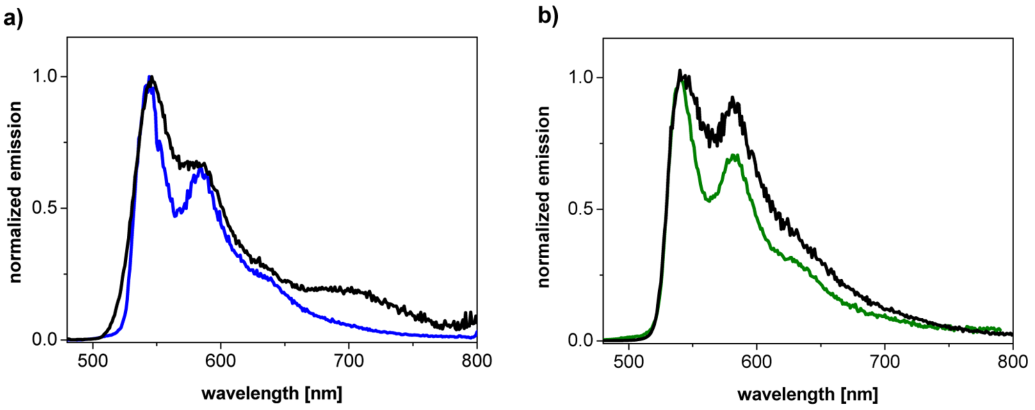

Figure 3. Normalized emission spectra of the binuclear species ($c \approx 5 \times 10^{-6}$ M) in comparison to related mononuclear complexes ($c \approx 10^{-5}$ M) in glassy DCM at 77 K: (a) binuclear complex **3a** (black line), λ_{ex} 430 nm, and mononuclear complex **M-3a** (blue line), λ_{ex} 400 nm; (b) binuclear compound **3b** (black line) and mononuclear complex **M-3b**/**8a** (green line), λ_{ex} 430 nm.

other three binuclear complexes with respect to their related mononuclear Pt^{II} analogues. The onsets of the first reversible reduction wave generally lay between −1.49 and −1.65 V vs the ferrocene/ferrocenium (Fc/Fc^+) couple and the onsets of the second reversible reduction wave between −2.14 and −2.21 V vs Fc/Fc^+. Both waves are due to single-electron reductions of the bipyridine ligand leading to stable radical anions and dianions, respectively.[3g,23] The reduction properties showed only negligible variations if measured in DCM instead of DMF.

The onsets of the irreversible oxidation waves of all complexes vary in the range 0.32−0.73 V vs Fc/Fc^+. In general, oxidation is attributed to the Pt^{II}/Pt^{III} process,[3g] which is irreversible due to the instability of the Pt^{III} species and their follow-up reactions such as reductive elimination.[30] While the oxidation onset of mononuclear complex **M-3a** occurs at 0.73 V vs Fc/Fc^+, the corresponding binuclear compound **3a** showed a distinctively lowered oxidation wave with an onset at 0.34 V vs Fc/Fc^+ in DMF. The oxidation of both complexes was also measured in DCM, where both values appeared slightly lowered with respect to the measurement in DMF (0.66 V for mononuclear complex **M-3a**, 0.32 V for binuclear complex **3a**).

Table 2. Wavelength-Dependent Excited-State Lifetime Analysis[a]

complex	λ_{em}	τ (ns)	rel amplitude	assignment
3a	600	222	0.018	noninteracting Pt^{II} centers
		3	0.805	interacting Pt^{II} centers
		29	0.176	excimer decay
3a	770	222	0.003	noninteracting Pt^{II} centers
		3	−0.173	interacting Pt^{II} centers (rise time)
		29	1.170	excimer decay
3b	600	186	0.060	noninteracting Pt^{II} centers
		104	0.620	weakly interacting Pt^{II} centers
		3	0.131	strongly interacting Pt^{II} centers
		27	0.189	excimer decay
3b	770	104	0.216	weakly interacting Pt^{II} centers
		3	−0.353	strongly interacting Pt^{II} centers (rise time)
		27	1.137	excimer decay
8a	590	287	0.097	noninteracting Pt^{II} centers
		83	0.423	weakly interacting Pt^{II} centers
		7	0.311	strongly interacting Pt^{II} centers
		29	0.168	excimer decay
8a	735	83	0.033	weakly interacting Pt^{II} centers
		7	−0.118	strongly interacting Pt^{II} centers (rise time)
		29	1.086	excimer decay
8b	590	610	0.015	noninteracting Pt^{II} centers
		210	0.112	weakly interacting Pt^{II} centers
		5	0.554	strongly interacting Pt^{II} centers
		34	0.319	excimer decay
8b	735	210	0.146	weakly interacting Pt^{II} centers
		5	−0.138	strongly interacting Pt^{II} centers (rise time)
		34	0.992	excimer decay

[a] Measurements were carried out in DCM, with $c[Pt] < 10^{-5}$ mol L^{-1}, at 298 K. The corresponding decays and fittings are shown in the Supporting Information (Figures S21−S36).

The oxidation of the more flexible binuclear Pt^{II} complex **3b** in comparison to the related mononuclear compound **M-3b/8a** yielded similar results if measured in DCM. The oxidation onset of the binuclear complex appeared at lower potential (0.37 V) with respect to the mononuclear compound. However, if the CVs were measured in DMF, the oxidation onsets of mononuclear (0.65 V) and binuclear (0.70 V) species were quite similar. Thus, the oxidation potential of binuclear Pt^{II} complex **3b** is shifted from 0.65 to 0.37 V by changing the solvent from DMF to DCM (Figure 4b). Likewise, the HOMO energy level of compound **3b** dropped from −5.75 to −5.47 eV vs vacuum, reducing the energy gap from 2.19 to 1.85 eV.

Binuclear compound **8a** showed oxidation behavior similar to that of derivative **3b**, displaying values comparable to those for the related mononuclear complex **M-3b/8a** in DMF solution. However, if one compares binuclear species **8a**,**b**, one can see that the oxidation onset of **8b** (which has no hexyl side chains at the phenylacetylide) is shifted to lower potentials by more than 200 mV. This effect might arise from steric hindrance and distortion of the ligand due to the hexyl side chains.

The electron-donating effect of the linker on the oxidation potential is negligible, as the HOMO is mainly located at the metal and the phenylacetylides.[23] However, the oxidation potentials drop with decreasing flexibility of the spacer within the binuclear systems. These observations suggest that the lowered oxidation potentials, and therefore the apparent lowered HOMO energy levels of the binuclear complexes, are due to the spatial proximity of adjacent Pt^{II} centers, as the mononuclear complexes do not show such behavior at the same Pt^{II} concentration. Thus, the observed Pt^{II}/Pt^{III} oxidation is influenced by intramolecular stabilization via Pt−Pt interactions. Such ground-state equilibria are not observable in the absorption and excitation spectra. Nevertheless, the electrochemical trends concerning the choice of solvent and steric aspects within the binuclear structure correlate with those observed in emission spectroscopy.

■ CONCLUSION

In this study, we have designed and synthesized a set of binuclear Pt^{II} complexes by decorating different bridging units via click chemistry employing adequately substituted mononuclear Pt^{II} coordination compounds. Steady-state and time-resolved emission spectroscopy proved intramolecular excimer formation. The proximity of the metal centers in the ground state, which cannot be traced by spectroscopic measurements, has been revealed with the aid of cyclic voltammetry. The binuclear Pt^{II} compounds displayed lowered oxidation potentials (Pt^{II}/Pt^{III}) in comparison to their related mononuclear complexes measured at the same Pt^{II} concentration. The solvent-dependent electrochemical behavior correlates well with the trends observed in the emission spectra. When the solvent is changed from DMF to DCM, for example, the emission color of binuclear Pt^{II} complexes and likewise their

Table 3. Electrochemical Parameters of the Mono- and Binuclear Pt^{II} Complexes

complex	solvent	E^{onset}_{ox}[a] (V)	E^{onset}_{red1}[a] (V)	E^{onset}_{red2}[a] (V)	E_{HOMO}[b] (eV)	E_{LUMO}[b] (eV)	E_g[c] (eV)
M-3a	DMF	0.73	−1.59	−2.20	−5.83	−3.52	2.31
M-3a	DCM	0.66	−1.57		−5.76	−3.53	2.23
M-3b/8a	DMF	0.70	−1.59	−2.19	−5.80	−3.51	2.29
M-8b	DMF	0.71	−1.54	−2.15	−5.81	−3.56	2.26
3a	DMF	0.34	−1.59	−2.18	−5.44	−3.51	1.93
3a	DCM	0.32	−1.65		−5.42	−3.45	1.98
3b	DMF	0.65	−1.55	−2.14	−5.75	−3.56	2.19
3b	DCM	0.37	−1.49		−5.47	−3.61	1.85
8a	DMF	0.62	−1.57	−2.21	−5.72	−3.53	2.19
8b	DMF	0.41	−1.56	−2.20	−5.51	−3.54	1.97

[a] Conditions: measured vs Fc/Fc^+ in DMF/DCM (0.1 M $TBAPF_6$), c(**M3a**, **M3b/8a**, and **M-8b**) = 10^{-3} M, c(**3a**,**b** and **8a**,**b**) = 5×10^{-4} M, 295 K, scan rate 100 mV s^{-1}. [b] Vs vacuum, determined from the onsets of oxidation and reduction waves, using the equation $E_{HOMO/LUMO} = -5.1\ eV - E^{onset}_{ox}/E^{onset}_{red1}$.[29] [c] Calculated by the difference of the values of E_{LUMO} and E_{HOMO}.

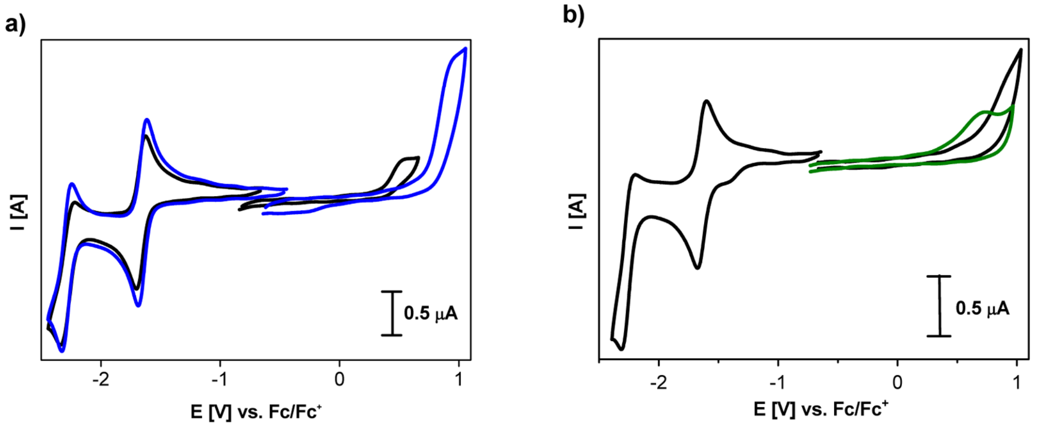

Figure 4. (a) Cyclic voltammograms (CVs) of binuclear Pt^{II} complex **3a** (black line; $c = 5 \times 10^{-4}$ M) and the corresponding mononuclear compound **M-3a** (blue line; $c = 10^{-3}$ M) in DMF (0.1 M TBAPF$_6$). (b) CVs of binuclear Pt^{II} complex **3b** ($c = 5 \times 10^{-4}$ M) in DMF (black line) and DCM (green line).

HOMO level are shifted to lower energies. Furthermore, the intramolecular Pt^{II}–Pt^{II} and π–π interactions are shown to decrease with the length and flexibility of the spacer, providing a design criterion for tailored photoactive materials.

EXPERIMENTAL SECTION

General Remarks on the Synthesis. *o*-Xylene, tetraethylene glycol, and 2-bromophenol were purchased from Merck, and 4-bromobenzyl bromide and iron pentacarbonyl were purchased from Acros. The catalyst tetrakis(acetonitile)copper(I) hexafluorophosphate, Cu(CH$_3$CN)$_4$PF$_6$, and deuterated solvents for NMR spectroscopy were purchased from Aldrich. 1,2-Bis(bromomethyl)benzene,[31] 1,3-bis(4-bromophenyl)propan-2-one (**4**),[25] and 1,13-bis(2-bromophenyl)-1,4,7,10,13-pentaoxatridecane (**6**)[27] were prepared according to literature-known protocols. The synthesis of mononuclear Pt^{II} complexes **M3a**, **M-3b**/**8a**, and **M-8b** is reported elsewhere.[23]

All solvents were purchased from Merck (VWR International) and were used as received for workup procedures, distilled for purification purposes, and dried for use in reactions according to standard protocols.[32] Column chromatography was performed with flash silica gel, particle size 0.04–0.064 mm, from Macherey-Nagel and basic aluminum oxide (alumina) "90" (particle size 0.04–0.064 mm) from Merck, respectively. The alumina was deactivated to "Brockmann" activity II-III, by adding 5% distilled water. Thin-layer chromatography was carried out on aluminum sheets coated with silica gel (Merck TLC silica gel 60 F$_{254}$) and aluminum oxide (Merck TLC aluminum oxide 150 F$_{254}$, neutral), respectively. Bio-Beads S-X1 (200–400 mesh) from BIO-RAD was used as the stationary phase for size exclusion chromategraphy (SEC).

Physicochemical, Electrochemical, and Photophysical Measurements. NMR spectra were recorded on a Bruker 400 spectrometer at 25 °C, unless noted otherwise. Chemical shift values (δ) are expressed in parts per million using residual solvent protons (CDCl$_3$, ^{1}H δ 7.26 ppm and ^{13}C δ 77.36 ppm; CD$_2$Cl$_2$, ^{1}H δ 5.33 ppm and ^{13}C δ 54.24 ppm)[33] as internal standard. The numbering of atoms herein is chosen due to practical aspects for the assignment of NMR signals and does not conform to IUPAC nomenclature. CI mass spectra were recorded on a Finnigan MAT SSQ-7000 instrument and MALDI mass spectra on a Bruker Daltonics Reflex III instrument. High-resolution mass spectra (HRMS) were measured using a Bruker solariX spectrometer and MALDI source. Melting points were determined using a Büchi B-545 apparatus. Elemental analyses were performed on an Elementar Vario EL instrument (Department of Analytical Chemistry, University of Ulm). IR spectroscopy was measured on a Perkin-Elmer FT-IR Spectrum 2000 instrument. Photophysical measurements were carried out in 1 cm cuvettes with Merck spectroscopic grade solvents. Absorption spectra were recorded on a Perkin-Elmer Lambda 19 spectrometer and emission spectra at room temperature on a Perkin-Elmer LS 55 spectrometer. The emission spectra were fully corrected for the photodetector response. Luminescence measurements at 77 K and excitation spectra were recorded with a Spex FluoroLog-3 spectrofluorometer (Horiba-Jobin-Yvon Inc.) equipped with a TBX detector or a Peltier-cooled photomultiplier (Hamamatsu R928) and double excitation and emission monochromators. The emission spectra were corrected for monochromator and detector efficiency and for the source intensity (450 W xenon lamp). Time-resolved measurements were carried out on an Edinburgh LifeSpec II spectrometer. An EPL laser diode (405 nm; FHWM < 80 ps) with repetition rates between 10 kHz and 1 MHz was used to excite the samples. The excitation sources were mounted directly on the sample chamber at 90° to a double-grating emission monochromator (5.4 nm/mm dispersion; 1200 grooves/mm blazed at 500 nm) and collected by a MCP-PMT (Hamamatsu R3809U-50) single-photon-counting detector. The photons collected at the detector are correlated by a time-to-amplitude converter (TAC) to the excitation pulse. Signals were collected using a TCC900 plug-in PC card for TCSPC with START and STOP CFDs, Variable Timing Delay, Time to Amplitude Converter (full range 2.5 ns to 50 μs), Flash ADC, and memory, and data analysis was performed using the commercially available F900 software (Edinburgh Instruments). Luminescence quantum yields were measured with a Hamamatsu Photonics absolute PL quantum yield measurement system (C9920-02) equipped with a L9799-01 CW xenon light source (150 W), monochromator (excitation wavelengths 250–700 nm, bandwidth fwhm 10 nm), C7473 photonic multichannel analyzer, and integrating sphere and employing U6039-05 PLQY measurement software (Hamamatsu Photonics, Ltd., Shizuoka, Japan). The detector is a PMA multichannel capable of simultaneously measuring multiple wavelengths that have been corrected for wavelength sensitivity.

Cyclic voltammetry experiments were performed with a computer-controlled Autolab PGSTAT30 potentiostat in a three-electrode single-compartment cell with a platinum working electrode, a platinum-wire counter electrode, and an Ag/AgCl reference electrode. All potentials were internally referenced to the ferrocene/ferrocenium (Fc/Fc$^+$) couple.

1,2-Bis(azidomethyl)benzene (1a).[24] A 0.5 M solution of sodium azide in dry DMSO was prepared (0.63 g, 9.7 mmol, NaN$_3$ in 19 mL of DMSO). The solution was stirred at room temperature for 20 h, and then 1,2-bis(bromomethyl)benzene (1.16 g, 4.4 mmol) was added. Stirring was continued at room temperature for 3 days. Water (50 mL) was added, and the solution became warm. After the solution was cooled to room temperature, it was extracted with diethyl ether (3 × 30 mL). The combined organic layers were washed with water (30 mL) and brine (30 mL). It was dried over Na$_2$SO$_4$, and the solvent was removed in vacuo. Product **1a** (0.79 g, 4.2 mmol, 95%) remained as a yellow oil. No further purification was needed. ^{1}H NMR (CDCl$_3$, 400 MHz): δ 4.44 (s, 4H, H-*benzyl*), 7.36–7.41 (m, 4H, H-*Ar*) ppm. ^{13}C

NMR ($CDCl_3$, 100 MHz): δ 52.6 (C-*benzyl*), 129.3 (C-3,6), 130.5 (C-4,5), 134.2 (C-1,2) ppm. R_f = 0.50 (silica, *n*-hexane/ethyl acetate 5/1). IR (NaCl; cm^{-1}): 2941 (m), 2887 (m), 2460 (w), 2096 (s, br), 1456 (m), 1347 (m), 1251 (s), 883 (m), 756 (m).

1,3-Bis(4-bromophenyl)propane (5). 1,3-Bis(4-bromophenyl)propan-2-one (**4**; 1.50 g, 4.08 mmol), powdered potassium hydroxide (0.91 g, 16.30 mmol), and hydrazine (0.74 mL, 12.23 mmol, 1.16 g, 80 wt % in water) were dissolved in triethylene glycol (40 mL). The solution was heated to 140 °C, and water (8 mL) was added. It was heated under reflux for 2 h. Then the water was distilled off and the solution was heated to 200 °C for 3.5 h. It was cooled to room temperature overnight. The mixture was poured into 2 N hydrochloric acid (150 mL) and DCM (100 mL). The layers were separated, and the aqueous layer was extracted with DCM (100 mL). The combined organic layers were washed with saturated sodium bicarbonate solution and water. The organic layer was dried over Na_2SO_4, the solvent was removed in vacuo, and the residue was purified via column chromatography using silica and petroleum ether (PE)/DCM 20/1. Product **5** (1.18 g, 3.34 mmol, 82%) was isolated as white crystals. Mp: 58−59 °C. ^{1}H NMR ($CDCl_3$, 400 MHz): δ 1.90 (qui, 2H, ^3J = 7.7 Hz, H-2), 2.58 (t, 4H, ^3J = 7.7 Hz, H-1,3), 7.04 (d, 4H, ^3J = 8.3 Hz, H-2′,6′), 7.40 (d, 4H, ^3J = 8.3 Hz, H-3′,5′) ppm. ^{13}C NMR ($CDCl_3$, 100 MHz): δ 32.9 (C-2), 35.0 (C-1,3), 119.9 (C-4′), 130.5 (C-2′,6′), 131.7 (C-3′,5′), 141.2 (C-1′) ppm. MS (CI, 100 eV): *m*/*z* 355 (100%, M + H$^+$), 277 (10%), 225 (6%), 197 (70%), 169 (20%), 119 (8%), 91 (11%). R_f = 0.50 (silica, PE). IR (KBr; cm^{-1}): 2939 (m), 2918 (m), 2857 (m), 1488 (s), 1460 (m), 1402 (m), 1070 (m), 1010 (m), 835 (m), 822 (m), 804 (s), 609 (m). Anal. Calcd for $C_{15}H_{14}Br_2$: C, 50.88; H, 3.99. Found: C, 51.03; H, 3.98.

1,3-Bis(4-azidophenyl)propane (1b). 1,3-Bis(4-bromophenyl)propane (**5**; 0.50 g, 1.41 mmol) was dissolved in ethanol (14 mL) and water (6 mL). The solution was degassed, and sodium azide (0.366 g, 5.63 mmol), sodium ascorbate (0.028 g, 0.14 mmol), CuI (0.054 g, 0.26 mmol), and DMEDA (0.05 mL, 0.42 mmol, 0.037 g) were added under argon. The mixture was heated under reflux for 4.5 h. Then, it was poured into water (30 mL) containing 25% ammonia (2 mL) and DCM (30 mL). After the mixture was stirred for some minutes, the layers were separated and the aqueous layer was extracted with DCM (30 mL). The combined organic layers were dried over Na_2SO_4, and the solvent was removed in vacuo. The residue was purified via column chromatography with silica and PE/DCM 10/1. Product **1b** (0.298 g, 1.072 mmol, 76%) was isolated as a yellow oil. ^{1}H NMR ($CDCl_3$, 400 MHz): δ 1.91 (qui, 2H, ^3J = 7.7 Hz, H-2), 2.61 (t, 4H, ^3J = 7.7 Hz, H-1,3), 6.95 (d, 4H, ^3J = 8.5 Hz, H-2′,6′), 7.15 (d, 4H, ^3J = 8.5 Hz, H-3′,5′) ppm. ^{13}C NMR ($CDCl_3$, 100 MHz): δ 33.3 (C-2), 35.0 (C-1,3), 119.3 (C-2′,6′), 130.1 (C-3′,5′), 137.9 (C-1′), 139.2 (C-4′) ppm. MS (CI, 100 eV): *m*/*z* 278 (9%, M$^+$), 251 (16%), 223 (100%), 196 (11%), 182 (5%), 132 (15%), 118 (19%), 106 (12%). R_f = 0.32 (silica, PE/DCM 10/1). IR (NaCl; cm^{-1}): 3027 (m), 2936 (m), 2858 (m), 2415 (m), 2254 (m), 2106 (s, br), 1606 (m), 1580 (m), 1506 (s), 1445 (m), 1288 (s, br), 1128 (m), 827 (m), 628 (m). Anal. Calcd for $C_{15}H_{14}N_6$: C, 64.73; H, 5.07; N, 30.20. Found: C, 64.79; H, 4.99; N, 30.25.

(*μ*-1,2-Bis{[4-(2,2′-bipyridin-5-yl)-1*H*-1,2,3-triazol-1-yl]methyl}benzene)tetrakis(4-hexylphenylethynyl)diplatinum(II) (3a). (TMS-ethynyl-bpy)Pt^{II} complex **2** (95.6 mg, 0.117 mmol) was dissolved in DCM (32 mL) and methanol (8 mL). KF (11 mg, 0.176 mmol) was added, and the solution was degassed. Diazide **1a** (11 mg, 0.058 mmol), $Cu(CH_3CN)_4PF_6$ (8.7 mg, 0.023 mmol), elemental copper (1 mg, 0.027 mmol), and DIPEA (0.04 mL, 0.23 mmol, 0.03 g) were added. Stirring was continued at room temperature for 2 days. The solution was diluted with DCM (100 mL) and washed with water (40 mL) containing 25% ammonia (10 mL) and subsequently with 0.1 M Na_2-EDTA solution (35 mL). It was dried over Na_2SO_4, and the solvent was removed in vacuo. The residue was purified via column chromatography with silica and DCM/diethyl ether 20/1. It was further purified via SEC with DCM as eluent and precipitated from DCM solution with PE. Product **3a** (82 mg, 0.049 mmol, 84%) was obtained as an orange powder. ^{1}H NMR (CD_2Cl_2, 400 MHz): δ 0.91−0.97 (m, 12H, H-12″), 1.36−1.46 (m, 24H, H-9″, H-10″, H-11″), 1.59−1.73 (m, 8H, H-8″), 2.63−2.68 (m, 8H, H-7″), 5.52 (s, 4H, H-*benzyl*), 7.00 (s, 2H, H-5‴), 7.10 + 7.17 (2 × d, 2 × 4H, ^3J = 8.1 Hz, H-5″), 7.35−7.38 (m, 10H, H-5′, H-4″), 7.53−7.57 (m, 2H, H-*A*-Ar), 7.66−7.70 (m, 2H, H-*B*-Ar), 7.75 (dd, 2H, ^3J = 8.3 Hz, ^4J = 1.8 Hz, H-3′), 7.80 (d, 2H, ^3J = 8.4 Hz, H-3′), 8.02−8.06 (m, 4H, H-4,4′), 9.12 (d, 2H, ^4J = 1.4 Hz, H-6), 9.14 (d, 2H, ^3J = 5.4 Hz, H-6′) ppm. MS (MALDI-TOF, dithranol): *m*/*z* 1679 (M$^+$), 1903 ([M + matrix]$^+$). R_f = 0.59 (silica, DCM/diethyl ether 25/1). IR (KBr; cm^{-1}): 2954 (m), 2925 (s), 2853 (m), 2113 (m), 1636 (m), 1606 (m), 1503 (m), 1466 (m), 826 (m). Anal. Calcd for $C_{88}H_{92}N_{10}Pt_2$: C, 62.92; H, 5.52; N, 8.34. Found: C, 62.81; H, 5.66; N, 8.27.

(*μ*-1,3-Bis{4-[4-(2,2′-bipyridine-5-yl)-1*H*-1,2,3-triazol-1-yl]-phenyl}propane)tetrakis(4-hexylphenylethynyl)diplatinum(II) (3b). (TMS-ethynyl-bpy)Pt^{II} complex **2** (57 mg, 0.070 mmol) was dissolved in DCM (32 mL) and methanol (8 mL). KF (5 mg, 0.105 mmol) was added, and the solution was degassed. Diazide **1b** (10 mg, 0.035 mmol), $Cu(CH_3CN)_4PF_6$ (5 mg, 0.014 mmol), elemental copper (1 mg, 0.014 mmol), and DIPEA (0.02 mL, 0.140 mmol, 0.02 g) were added. The synthesis and purification were carried out as described above for compound **3a**. Product **3b** (47 mg, 0.027 mmol, 77%) was isolated as an orange powder. ^{1}H NMR (CD_2Cl_2, 400 MHz): δ 0.92−0.95 (m, 12H, H-12″), 1.32−1.44 (m, 24H, H-9″, H-10″, H-11″), 1.64−1.73 (m, 8H, H-8″), 2.22−2.26 (m, 2H, H-2⁗), 2.64−2.69 (m, 8H, H-7″), 2.87 (t, 4H, ^3J = 6.0 Hz, H-1⁗,3⁗), 7.13−7.19 (m, 12H, H-*o*-Ar, H-5″), 7.30−7.32 + 7.48−7.50 (2 × m, 10H, H-4″, H-5′), 7.40 (d, 4H, ^3J = 7.9 Hz, H-*m*-Ar), 7.95 (s, 2H, H-5‴), 8.02−8.06 (m, 2H, H-4′), 8.24 (d, 2H, ^3J = 8.1 Hz, H-3′), 8.31 (d, 2H, ^3J = 8.2 Hz, H-3), 8.49−8.51 (m, 2H, H-4), 9.19 (d, 2H, ^3J = 4.4 Hz, H-6′), 9.77 (s, 2H, H-6) ppm. MS (MALDI-TOF, dithranol): *m*/*z* 1770 (M$^+$), 1993 ([M + matrix]$^+$). R_f = 0.30 (silica, DCM/diethyl ether 20/1). IR (KBr; cm^{-1}): 2953 (m), 2924 (s), 2853 (m), 2112 (m), 1635 (m), 1605 (m), 1519 (m), 1504 (m), 1467 (m), 1237 (m), 1032 (m), 826 (m), 785 (m). Anal. Calcd for $C_{95}H_{98}N_{10}Pt_2$: C, 64.46; H, 5.58; N, 7.91. Found: C, 64.06; H, 5.78; N, 7.74.

(*μ*-1,13-Bis{2-[4-(2,2′-bipyridin-5-yl)-1*H*-1,2,3-triazol-1-yl]-phenyl}-1,4,7,10,13-pentaoxatridecane)tetrakis(4-hexylphenylethynyl)diplatinum(II) (8a). 1,13-Bis(2-bromophenyl)-1,4,7,10,13-pentaoxatridecane (**6**; 0.16 g, 0.317 mmol) was dissolved in dry THF (2 mL) under argon. The solution was cooled to −78 °C, and *n*-butyllithium (0.38 mL, 0.793 mmol, 2.5 M in *n*-hexane) was added dropwise. Stirring was continued at −78 °C for 45 min. Tosyl azide (0.188 g, 0.951 mmol) was added, and stirring was continued at −70 °C for 5 h. The solution was warmed to −20 °C, and diethyl ether (10 mL) and 0.1 M aqueous disodium phosphate solution (10 mL) were added. Stirring was continued vigorously at room temperature for 15 min. The layers were separated, and the aqueous layer was extracted with diethyl ether (3 × 50 mL). The combined organic layers were washed with 0.1 M Na_2-EDTA solution and dried over $MgSO_4$. The solvent was removed in vacuo, and the residue was purified via column chromatography with silica and PE/ethyl acetate 1/1. A yellow oil (90 mg) of a 6/1 mixture of the azido substituted product 1,13-bis(2-azidophenyl)-1,4,7,10,13-pentaoxatridecane and the mono-/dihydrogenated byproducts was obtained (quantified via ^{1}H NMR), which could not be separated via column chromatography.[28] ^{1}H NMR ($CDCl_3$, 400 MHz; chemical shifts and integrals of the byproduct are given in brackets): δ 3.68−3.74 (m, 8H, H-5,9, H-6,8), 3.86−3.89 [3.84−3.87] (m, 4H, H-3,11), 4.12−4.19 [4.11−4.13] (m, 4H [0.64H], H-2,12), 6.89−6.97 (m, 6H, H-4′, H-5′, H-6′), 7.04−7.08 [7.25−7.29] (m, 2H, H-3′) ppm. This mixture (7.3 mg, ∼0.017 mmol) was dissolved together with (ethynyl-bpy)Pt^{II} complex **7a** (25 mg, 0.034 mmol) in DCM (28 mL) and methanol (7 mL) under argon, and the solution was degassed. $Cu(CH_3CN)_4PF_6$ (2.5 mg, 0.007 mmol), elemental copper (1 mg, 0.007 mmol), and DIPEA (0.01 mL, 0.068 mmol, 9 mg) were added. Stirring was continued at room temperature for 8 days. The workup and purification were carried out as described above for compound **3a**. Product **8a** (9 mg, 0.005 mmol, 19% with respect to **6**) was isolated as an orange powder. ^{1}H NMR ($CDCl_3$, 400 MHz): δ 0.89−0.93 (m, 12H, H-12″), 1.31−1.38 (m, 24H, H-9″, H-10″, H-11″), 1.52−1.65 (m, 8H, H-8″), 2.50−2.59 (m, 8H, H-7″), 3.54−3.61 (m, 8H, H-5⁗,9⁗, H-6⁗,8⁗), 3.68−3.70 (m, 4H, H-3⁗,11⁗), 3.93−3.95

(m, 4H, H-2′′′′,12′′′′), 6.87 (d, 2H, ^{3}J = 8.2 Hz, H-*o*-Ar), 6.98−7.01 (m, 8H, H-5″), 7.05 (t, 2H, ^{3}J = 7.8 Hz, H-*p*-Ar), 7.19−7.22 (m, 2H, H-5′), 7.26 + 7.47 (2 × d, 2 × 4H, ^{3}J = 8.0 Hz, H-4″), 7.30−7.34 (m, 2H, H-m_1-Ar), 7.69 (td, 2H, ^{3}J = 8.1 Hz, ^{4}J = 1.2 Hz, H-4′), 7.79 (dd, 2H, ^{3}J = 7.8 Hz, ^{4}J = 1.4 Hz, H-m_2-Ar), 8.04 (d, 2H, ^{3}J = 8.1 Hz, H-3′), 8.16 (d, 2H, ^{3}J = 8.5 Hz, H-3), 8.38 (dd, 2H, ^{3}J = 8.4 Hz, ^{4}J = 1.9 Hz, H-4), 8.59 (s, 2H, H-5‴), 9.29 (d, 2H, ^{3}J = 5.4 Hz, H-6′), 9.79 (d, 2H, ^{4}J = 1.7 Hz, H-6) ppm. HRMS (MALDI-TOF, dithranol): *m/z* 1920.79075 ($C_{100}H_{108}N_{10}O_5Pt_2$); calcd 1920.78911 ($C_{100}H_{108}N_{10}O_5Pt_2$). R_f = 0.48 (silica, DCM/diethyl ether 25:1). IR (KBr; cm^{-1}): 2953 (m), 2925 (m), 2854 (m), 2114 (m), 1636 (m), 1605 (m), 1504 (s), 1467 (m), 1248 (m), 1115 (m), 1028 (m), 751 (m).

(*μ*-1,13-Bis{2-[4-(2,2′-bipyridin-5-yl)-1*H*-1,2,3-triazol-1-yl]-phenyl}-1,4,7,10,13-pentaoxatridecane)tetrakis(phenylethynyl)diplatinum(II) (8b). Crude 1,13-bis(2-azidophenyl)-1,4,7,10,13-pentaoxatridecane (22.3 mg, ∼0.052 mmol) obtained from the synthesis described for **8a** was dissolved together with (ethynyl-bpy)Pt^{II} complex **7b** (60 mg, 0.104 mmol) in DCM (40 mL) and methanol (10 mL) under argon, and the solution was degassed. $Cu(CH_3CN)_4PF_6$ (7.8 mg, 0.021 mmol), elemental copper (1.3 mg, 0.021 mmol), and DIPEA (0.035 mL, 0.208 mmol, 0.027 g) were added. Stirring was continued at room temperature for 8 days. Workup and purification were carried out as described above for compound **3a**. Product **8b** (20 mg, 0.013 mmol, 17% with respect to **6**) was isolated as an orange powder. ^{1}H NMR ($CDCl_3$, 400 MHz): δ 3.51−3.60 (m, 8H, H-5′′′′,9′′′′, H-6′′′′,8′′′′), 3.64−3.66 (m, 4H, H-3′′′′,11′′′′), 3.89−3.91 (m, 4H, H-2′′′′,12′′′′), 6.81 (d, 2H, ^{3}J = 8.2 Hz, H-*o*-Ar), 6.99 (t, 2H, ^{3}J = 7.7 Hz, H-*p*-Ar), 7.06−7.11 (m, 4H, H-6″), 7.15−7.20 (m, 10H, H-5″, H-m_1-Ar), 7.24−7.28 (m, 2H, H-5′), 7.33 + 7.53 (2 × d, 2 × 4H, ^{3}J = 7.1 Hz, H-4″), 7.67 (td, 2H, ^{3}J = 8.1 Hz, ^{4}J = 1.3 Hz, H-4′), 7.74 (dd, 2H, ^{3}J = 7.8 Hz, ^{4}J = 1.4 Hz, H-m_2-Ar), 7.93 (d, 2H, ^{3}J = 8.0 Hz, H-3′), 8.05 (d, 2H, ^{3}J = 8.5 Hz, H-3), 8.28 (dd, 2H, ^{3}J = 8.4 Hz, ^{4}J = 1.9 Hz, H-4), 8.49 (s, 2H, H-5‴), 9.22 (d, 2H, ^{3}J = 5.2 Hz, H-6′), 9.67 (d, 2H, ^{4}J = 1.7 Hz, H-6) ppm. HRMS (MALDI-TOF, dithranol): *m/z* 1583.41285 ($C_{76}H_{60}N_{10}O_5Pt_2$); calcd 1583.41123 ($C_{76}H_{60}N_{10}O_5Pt_2$). R_f = 0.16 (silica, DCM/diethyl ether 25/1). IR (KBr; cm^{-1}): 2925 (m), 2870 (m), 2113 (s), 1635 (s), 1604 (s), 1506 (m), 1486 (s), 1467 (m), 1248 (m), 1129 (m), 1029 (m), 756 (m), 695 (m).

■ ASSOCIATED CONTENT

Ⓢ Supporting Information

Figures giving additional absorption, emission, and excitation spectra, decays and fittings of the lifetime analysis, and cyclic voltammograms and proton NMR spectra of the complexes. This material is available free of charge via the Internet at http://pubs.acs.org.

■ AUTHOR INFORMATION

Corresponding Authors

*E-mail for L.D.C.: decola@unistra.fr.
*E-mail for P.B.: peter.baeuerle@uni-ulm.de.

Present Address

∥Institut de Science et d'Ingénierie Supramoléculaires (I.S.I.S.), Université de Strasbourg, 8 allée Gaspard Monge, 67000 Strasbourg, France.

Notes

The authors declare no competing financial interest.

■ ACKNOWLEDGMENTS

We thank the Dutch Polymer Institute (DPI) for funding this project. This research formed part of the research programme of the DPI, project #628.

■ REFERENCES

(1) Cyclometalated ligands: (a) Chassot, L.; Müller, E.; von Zelewsky, A. *Inorg. Chem.* **1984**, *23*, 4249−4253. (b) Clark, M. K.; Diring, S.; Retailleau, P.; McMillin, D. R.; Ziessel, R. *Chem. Eur. J.* **2008**, *14*, 7168−7179. (c) Shao, P.; Li, Y.; Azenkeng, A.; Hoffmann, M. R.; Sun, W. *Inorg. Chem.* **2009**, *48*, 2407−2419. (d) Schneider, J.; Du, P.; Jarosz, P.; Lazarides, T.; Wang, X.; Brennessel, W. W.; Eisenberg, R. *Inorg. Chem.* **2009**, *48*, 4306−4317. (e) Rausch, A. F.; Murphy, L.; Williams, J. A. G.; Yersin, H. *Inorg. Chem.* **2009**, *48*, 11407−11414. (f) Rausch, A. F.; Monkowius, U. V.; Zable, M.; Yersin, H. *Inorg. Chem.* **2010**, *49*, 7818−7825. (g) Fuertes, S.; Brayshaw, S. K.; Raithby, P. R.; Schiffers, S.; Warren, M. R. *Organometallics* **2012**, *31*, 105−119.

(2) Terpyridine ligands: (a) Büchner, R.; Field, J. S.; Haines, R. J.; Cunningham, C. T.; McMillin, D. R. *Inorg. Chem.* **1997**, *36*, 3952−3956. (b) Yam, V. W.-W.; Teng, R. P.-L.; Wong, K. M.-C.; Cheung, K.-K. *Organometallics* **2001**, *20*, 4476−4482. (c) Yang, Q.-Z.; Wu, L.-Z.; Wu, Z.-X.; Zhang, L.-P.; Tung, C.-H. *Inorg. Chem.* **2002**, *41*, 5653−5655.

(3) Bipyridine ligands: (a) Morgan, G. T.; Burstall, F. H. *J. Chem. Soc.* **1934**, 965−971. (b) Miskowski, V. M.; Houlding, V. H.; Che, C.-M.; Wang, Y. *Inorg. Chem.* **1993**, *32*, 2518−2524. (c) Chan, C.-W.; Cheng, L.-K.; Che, C.-M. *Coord. Chem. Rev.* **1994**, *132*, 87−97. (d) James, S. L.; Younus, M.; Raithby, P. R.; Lewis, J. *J. Organomet. Chem.* **1997**, *543*, 233−235. (e) Hissler, M.; Connick, W. B.; Geiger, D. K.; McGarrah, J. E.; Lipa, D.; Lachicotte, R. J.; Eisenberg, R. *Inorg. Chem.* **2000**, *39*, 447−457. (f) Whittle, C. E.; Weinstein, J. A.; George, M. W.; Schanze, K. S. *Inorg. Chem.* **2001**, *40*, 4053−4062. (g) Chan, S.-C.; Chan, M. C. W.; Wang, Y.; Che, C.-M.; Cheung, K.-K.; Zhu, N. *Chem. Eur. J.* **2001**, *7*, 4180−4190. (h) Hua, F.; Kinayyigit, S.; Cable, J. R.; Castellano, F. N. *Inorg. Chem.* **2005**, *44*, 471−473. (i) Castellano, F. N.; Pomestchenko, I. E.; Shikhova, E.; Hua, F.; Muro, M. L.; Rajapakse, N. *Coord. Chem. Rev.* **2006**, *250*, 1819−1828. (j) Hua, F.; Kinayyigit, S.; Cable, J. R.; Castellano, F. N. *Inorg. Chem.* **2006**, *45*, 4304−4306. (k) Hua, F.; Kinayyigit, S.; Rachford, A. A.; Shikhova, E. A.; Goeb, S.; Cable, J. R.; Adams, C. J.; Kirschbaum, K.; Pinkerton, A. A.; Castellano, F. N. *Inorg. Chem.* **2007**, *46*, 8771−8783. (l) Ni, J.; Zhang, X.; Wu, Y.-H.; Zhang, L.-Y.; Chen, Z.-N. *Chem. Eur. J.* **2011**, *17*, 1171−1183. (m) Ni, J.; Zhang, X.; Qiu, N.; Wu, Y.-H.; Zhang, L.-Y.; Zhang, J.; Chen, Z.-N. *Inorg. Chem.* **2011**, *50*, 9090−9096. (n) Li, Y.; Tam, A. Y.-Y.; Wong, K. M.-C.; Wen, L.; Wu, L.; Yam, V. W.-W. *Chem. Eur. J.* **2011**, *17*, 8048−8059.

(4) Reviews: (a) Williams, J. A. G. *Top. Curr. Chem.* **2007**, *281*, 205−268. (b) Murphy, L.; Williams, J. A. G. *Top. Organomet. Chem.* **2010**, *28*, 75−111.

(5) (a) Baldo, M. A.; O'Brien, D. F.; You, Y.; Shoustikov, A.; Sibley, S.; Thompson, M. E.; Forrest, S. R. *Nature* **1998**, *395*, 151−154. (b) Kwong, R. C.; Sibley, S.; Dubovoy, T.; Baldo, M.; Forrest, S. R. *Chem. Mater.* **1999**, *11*, 3709−3713. (c) *Highly Efficient OLEDs with Phosphorescent Materials*, 1st ed.; Yersin, H., Ed.; Wiley-VCH: Weinheim, Germany, 2007. (d) Vezzu, D. A. K.; Deaton, J. C.; Jones, J. S.; Bartolotti, L.; Harris, C. F.; Marchetti, A. P.; Kondakova, M.; Pike, R. D.; Huo, S. *Inorg. Chem.* **2010**, *49*, 5107−5119. (e) Zhou, G.; Wang, Q.; Wang, X.; Ho, C.-L.; Wong, W.-Y.; Ma, D.; Wang, L.; Lin, Z. *J. Mater. Chem.* **2010**, *20*, 7472−7484.

(6) (a) Textor, M.; Oswald, H. R. *Z. Anorg. Allg. Chem.* **1974**, *407*, 244−256. (b) Miskowski, V. M.; Houlding, V. H. *Inorganic Chemistry* **1989**, *28*, 1529−1533. (c) Che, C.-M.; He, L.-Y.; Poon, C.-K.; Mak, T. C. W. *Inorg. Chem.* **1989**, *28*, 3081−3083. (d) Houlding, V. H.; Miskowski, V. M. *Coord. Chem. Rev.* **1991**, *111*, 145−152. (e) Miskowski, V. M.; Houlding, V. H. *Inorg. Chem.* **1991**, *30*, 4446−4452. (f) Miskowski, V. M.; Houlding, V. H.; Che, C.-M.; Wang, Y. *Inorg. Chem.* **1993**, *32*, 2518−2524. (g) Connick, W. B.; Henling, L. M.; Marsh, R. E.; Gray, H. B. *Inorg. Chem.* **1996**, *35*, 6261−6265.

(7) Bailey, J. A.; Hill, M. G.; Marsh, R. E.; Miskowski, V. M.; Schaefer, W. P.; Gray, H. B. *Inorg. Chem.* **1995**, *34*, 4591−4599.

(8) (a) Kunkely, H.; Vogler, A. *J. Am. Chem. Soc.* **1990**, *112*, 5625−5627. (b) Wan, K.-T.; Che, C.-M.; Cho, K.-C. *J. Chem. Soc., Dalton*

Trans. **1991**, 1077−1080. (c) Connick, W. B.; Geiger, D.; Eisenberg, R. *Inorg. Chem.* **1999**, *38*, 3264−3265. (d) Delahaye, S.; Loosli, C.; Liu, S.-X.; Decurtins, S.; Labat, G.; Neels, A.; Loosli, A.; Ward, T. R.; Hauser, A. *Adv. Funct. Mater.* **2006**, *16*, 286−295. (e) Pettijohn, C. N.; Jochnowitz, E. B.; Chuong, B.; Nagle, J. K.; Vogler, A. *Coord. Chem. Rev.* **1998**, *171*, 85−92.

(9) Kui, S. C. F.; Chow, P. K.; Tong, G. S. M.; Lai, S.-L.; Cheng, G.; Kwok, C.-C.; Low, K.-H.; Ko, M. Y.; Che, C.-M. *Chem. Eur. J.* **2013**, *19*, 69−73.

(10) (a) Yip, H.-K.; Che, C.-M.; Zhou, Z.-Y.; Mak, T. C. W. *J. Chem. Soc., Chem. Commun.* **1992**, 1369−1371. (b) Bailey, J. A.; Miskowski, V. M.; Gray, H. B. *Inorg. Chem.* **1993**, *32*, 369−370. (c) Bailey, J. A.; Gray, H. B. *Acta Crystallogr.* **1992**, *C48*, 1420−1422. (d) Bailey, J. A.; Miskowski, V. M.; Gray, H. B. *Acta Crystallogr.* **1993**, *C49*, 793−796.

(11) Sicilia, V.; Forniés, J.; Casas, J. M.; Martín, A.; López, J. A.; Larraz, C.; Pilar, B.; Ovejero, C.; Tordera, D.; Bolink, H. *Inorg. Chem.* **2012**, *51*, 3427−3435.

(12) (a) Koshiyama, T.; Omura, A.; Kato, M. *Chem. Lett.* **2004**, *33*, 1386−1387. (b) Saito, K.; Hamada, Y.; Takahashi, H.; Koshiyama, T.; Kato, M. *Jpn. J. Appl. Phys.* **2005**, *44*, L500−L501. (c) Ma, B.; Li, J.; Djurovich, P. I.; Yousufuddin, M.; Bau, R.; Thompson, M. E. *J. Am. Chem. Soc.* **2005**, *127*, 28−29. (d) Ma, B.; Djurovich, P. I.; Garon, S.; Alleyne, B.; Thompson, M. E. *Adv. Funct. Mater.* **2006**, *16*, 2438−2446. (e) Wang, K.-W.; Chen, J.-L.; Cheng, Y.-M.; Chung, M.-W.; Hsieh, C.-C.; Lee, G.-H.; Chou, P.-T.; Chen, K.; Chi, Y. *Inorg. Chem.* **2010**, *49*, 1372−1383.

(13) (a) Utsuno, M.; Yutaka, T.; Murata, M.; Kurihara, M.; Tamai, N.; Nishihara, H. *Inorg. Chem.* **2007**, *46*, 11291−11296. (b) Develay, S.; Williams, J. A. G. *Dalton Trans.* **2008**, 4562−4564. (c) Guo, Z.; Chan, M. C. W. *Chem. Eur. J.* **2009**, *15*, 12585−12588. (d) Munoz-Rodríguez, R.; Bunuel, E.; Williams, J. A. G.; Cárenas, D. J. *Chem. Commun.* **2012**, *48*, 5980−5982.

(14) Lai, S.-W.; Lam, H.-W.; Lu, W.; Cheung, K.-K.; Che, C.-M. *Organometallics* **2002**, *21*, 226−234.

(15) (a) Lu, W.; Chan, M. C. W.; Zhu, N.; Che, C.-M.; Li, C.; Hui, Z. *J. Am. Chem. Soc.* **2004**, *126*, 7639−7651. (b) Lai, S.-W.; Che, C.-M. *Top. Curr. Chem.* **2004**, *241*, 27−63. (c) Sun, W.; Zhu, H.; Barron, P. M. *Chem. Mater.* **2006**, *18*, 2602−2610. (d) Kui, S. C. F.; Chui, S. S.-Y.; Che, C.-M.; Zhu, N. *J. Am. Chem. Soc.* **2006**, *128*, 8297−8309. (e) Kui, S. C. F.; Sham, I. H. T.; Cheung, C. C. C.; Ma, C. W.; Yan, B.; Zhu, N.; Che, C.-M.; Fu, W.-F. *Chem. Eur. J.* **2007**, *13*, 417−435.

(16) Jamali, S.; Czerwieniec, R.; Kia, R.; Jamshidi, Z.; Zabel, M. *Dalton Trans.* **2011**, *40*, 9123−9130.

(17) (a) Yam, V. W.-W.; Chan, K. H.-Y.; Wong, K. M.-C.; Chu, B. W.-K. *Angew. Chem., Int. Ed.* **2006**, *45*, 6169−6173. (b) Kajitani, Y.; Tsuge, K.; Sasaki, Y.; Kato, M. *Chem. Eur. J.* **2012**, *18*, 11196−11200.

(18) Luo, J.; Liu, Y.; Chen, Q.; Shi, D.; Huang, Y.; Yu, J.; Wang, Y.; Zhang, Z.; Lei, G.; Zhu, W. *Dalton Trans.* **2013**, *42*, 1231−1237.

(19) (a) Camerel, F.; Ziessel, R.; Donnio, B.; Bourgogne, C.; Guillon, D.; Schmutz, M.; Iacovita, C.; Bucher, J.-P. *Angew. Chem., Int. Ed.* **2007**, *46*, 2659−2662. (b) Lu, W.; Chen, Y.; Roy, V. A. L.; Chui, S. S.-Y.; Che, C.-M. *Angew. Chem., Int. Ed.* **2009**, *48*, 7621−7626. (c) Wong, K. M.-C.; Yam, V. W.-W. *Acc. Chem. Res.* **2011**, *44*, 424−434. (d) Yeung, M. C.-L.; Yam, V. W.-W. *Chem. Eur. J.* **2011**, *17*, 11987−11990. (e) Hu, Y.; Chan, K. H.-Y.; Chung, C. Y.-S.; Yam, V. W.-W. *Dalton Trans.* **2011**, *40*, 12228−12234. (f) Strassert, C. A.; Chien, C.-H.; Galvez Lopez, M. D.; Kourkoulos, D.; Hertel, D.; Meerholz, K.; De Cola, L. *Angew. Chem., Int. Ed.* **2011**, *50*, 946−950. (g) Chang, K.-C.; Lin, J.-L.; Shen, Y.-T.; Hung, C.-Y.; Chen, C.-Y.; Sun, S.-S. *Chem. Eur. J.* **2012**, *18*, 1312−1321. (h) Moriuchi, T.; Sakamoto, Y.; Noguchi, S.; Fujiwara, T.; Akine, S.; Nabeshima, T.; Hirao, T. *Dalton Trans.* **2012**, *41*, 8524−8531. (i) Allampally, N. K.; Strassert, C. A.; De Cola, L. *Dalton Trans.* **2012**, *41*, 13132−13137. (j) Chen, Y.; Lu, W.; Che, C.-M. *Organometallics* **2013**, *32*, 350−353.

(20) (a) Koo, C.-K.; Lam, B.; Leung, S.-K.; Lam, M. H.-W.; Wong, W.-Y. *J. Am. Chem. Soc.* **2006**, *128*, 16434−16435. (b) Koo, C.-K.; Wong, K.-L.; Lau, K.-C.; Wong, W.-Y.; Lam, M. H.-W. *Chem. Eur. J.* **2009**, *15*, 7689−7698.

(21) (a) Leung, S. Y.-L.; Tam, A. Y.-Y.; Tao, C.-H.; Chow, H. S.; Yam, V. W.-W. *J. Am. Chem. Soc.* **2012**, *134*, 1047−1056. (b) Gross, A.; Moriuchi, T.; Hirao, T. *Chem. Commun.* **2013**, *49*, 1163−1165.

(22) (a) Kolb, H. C.; Finn, M. G.; Sharpless, K. B. *Angew. Chem., Int. Ed.* **2001**, *40*, 2004−2021. (b) Rostovtsev, V. V.; Green, L. G.; Fokin, V. V.; Sharpless, K. B. *Angew. Chem., Int. Ed.* **2002**, *41*, 2596−2599. (c) Tornoe, C. W.; Christensen, C.; Meldal, M. *J. Org. Chem.* **2002**, *67*, 3057−3064. (d) Bock, V. D.; Hiemstra, H.; van Maarseveen, J. H. *Eur. J. Org. Chem.* **2006**, 51−68.

(23) Stengel, I.; Strassert, C. A.; Plummer, E. A.; Chien, C.-H.; De Cola, L.; Bäuerle, P. *Eur. J. Inorg. Chem.* **2012**, *11*, 1795−1809.

(24) (a) Abu-Orabi, S. T.; Harmon, R. E. *J. Chem. Eng. Data* **1986**, *31*, 379−380. (b) Alvarez, S. G.; Alvarez, M. T. *Synthesis* **1997**, 413−414. (c) Ramírez-López, P.; de la Torre, M. C.; Montenegro, H. E.; Asenjo, M.; Sierra, M. A. *Org. Lett.* **2008**, *10*, 3555−3558.

(25) Ito, S.; Wehmeier, M.; Brand, J. D.; Kübel, C.; Epsch, R.; Rabe, J. P.; Müllen, K. *Chem.—Eur. J.* **2000**, *6*, 4327−4342.

(26) Method adopted from: Andersen, J.; Madsen, U.; Björkling, F.; Liang, X. *Synlett* **2005**, 2209−2213.

(27) Virtue, G. A.; Coyne, N. E.; Hamilton, D. G. *J. Org. Chem.* **2002**, *67*, 6856−6859.

(28) Procedure analogous to: Grigorenko, N. A.; Leumann, C. J. *Chem. Eur. J.* **2009**, *15*, 639−645.

(29) Zacharias, P.; Gather, M. C.; Rojahn, M.; Nuyken, O.; Meerholz, K. *Angew. Chem., Int. Ed.* **2007**, *46*, 4388−4392.

(30) Fuhrmann, G. L. Dissertation, Universität Ulm, 2006.

(31) Minsky, A.; Rabinovitz, M. *Synth. Commun.* **1983**, 497−498.

(32) Armarego, W. L. F.; Chai, C. L. L. *Purification of Laboratory Chemicals*, 5th ed.; Elsevier Science: Amsterdam, 2003.

(33) Fulmer, G. R.; Miller, A. J. M.; Sherden, N. H.; Gottlieb, H. E.; Nudelman, A.; Stoltz, B. M.; Bercaw, J. E.; Goldberg, K. I. *Organometallics* **2010**, *29* (9), 2176−2179.